ORGANIC CHEMISTRY FRONTIERS

RESEARCH ARTICLE

View Article Online
View Journal | View Issue

Cite this: *Org. Chem. Front.*, 2025, **12**, 42

Intermediate diradical character and thermal *cis–trans* isomerization of near-infrared absorbing thionated squaraine dyes†‡

Taishi Oka,[a] Takeshi Maeda, *[a] Daisuke Sakamaki, [b] Naoya Suzuki, [a] Shigeyuki Yagi, [a] Shintaro Kodama [a] and Hideki Fujiwara *[b]

Received 17th September 2024,
Accepted 21st October 2024

DOI: 10.1039/d4qo01722f

rsc.li/frontiers-organic

We synthesized squaraine dyes incorporating 4-membered thionated oxocarbon and chalcogenopyrylium moieties, which displayed intermediate diradical character as confirmed by bond-length analysis and temperature-dependent behaviors observed in ^{1}H NMR and ESR spectroscopy. The ^{1}H NMR signals of the cyclobutenedithione dyes disappeared at lower temperatures compared to the cyclobutenedione analogues, indicating a lower thermal transition to the excited triplet state and thus greater diradical character. Moreover, we identified *cis–trans* isomerization in the thionated dyes. Notably, an increase in diradical character lowered the activation energy of this isomerization, facilitating the structural transition between *cis* and *trans* isomers. These dyes exhibit strong near-infrared absorption, with slight temperature-dependent shifts likely arising from the closely matched electronic transition energies of the isomers.

Introduction

Singlet diradicaloids are molecules characterized by intermediate diradical character, which is illustrated by resonance structures that include both closed-shell and open-shell forms.[1–3] In these molecules, two electrons with antiparallel spins are only partially coupled in the ground state. This partial coupling causes the electrons to occupy separate spatial regions to minimize electron repulsion, thereby reducing the covalent character of the π bond and stabilizing the diradical resonance forms. As a result, singlet diradicaloids can facilitate thermal excitation from singlet to triplet states.[4–7] Over the past two decades, various stable singlet diradicaloids have been demonstrated, including π-extended quinodimethanes like Chichibabin's hydrocarbon,[8–10] quinoidal oligothiophenes,[11–13] and graphene fragments.[14,15] These compounds have attracted significant interest due to their unique physical properties stemming from diradical forms, which offer substantial potential for applications in nonlinear optics, singlet fission, and semiconductor materials.[16–19]

The diradical character not only influences the physical properties of these molecules but also affects their structural conversions. For instance, some singlet diradicaloids induced structural transformations through diradical configurations (Fig. 1A).[20] Kozaki, Okada, *et al.* reported the thermal *cis–trans* isomerization of a dithienoquinoid analogue of Chichibabin's hydrocarbon (Fig. 1B).[21] More recently, Wu *et al.* reported that oxindolyl-based Chichibabin's hydrocarbons induced *cis–trans* isomerization due to the contribution of the diradical forms

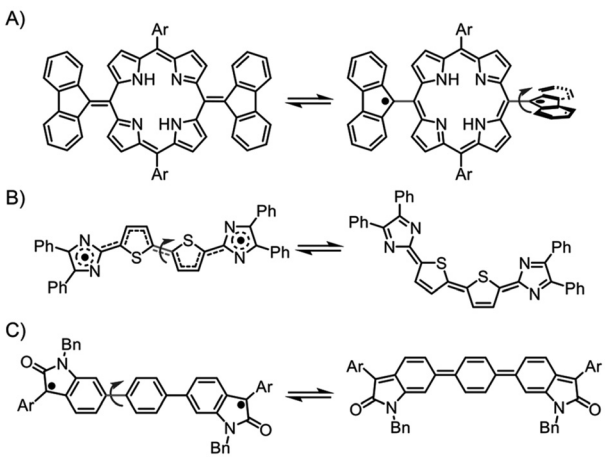

Fig. 1 An example of a structural change in a diradical form (A). Thermal *cis–trans* isomerization of Chichibabin's hydrocarbon analogues (B and C).

[a]*Department of Applied Chemistry, Graduate School of Engineering, Osaka Metropolitan University, Naka-ku, Sakai 599-8531, Japan. E-mail: tmaeda@omu.ac.jp*
[b]*Department of Chemistry, Graduate School of Science, Osaka Metropolitan University, Sumiyoshi-ku, Osaka 558-8585, Japan. E-mail: hfuji@omu.ac.jp*

† Dedicated to Prof. Dr Frank Würthner on the occasion of his 60th birthday.

‡ Electronic supplementary information (ESI) available. CCDC 2194625 and 2194626. For ESI and crystallographic data in CIF or other electronic format see DOI: https://doi.org/10.1039/d4qo01722f

(Fig. 1C).[22] These cases collectively highlight the pivotal role of intermediate diradical character in driving dynamic structural changes.

Until recently, the range of compounds classified as singlet diradicals was relatively narrow. However, it is now clear that a variety of compounds with extended π-electron systems exhibit sustained singlet diradical character. In fact, even molecules traditionally considered as closed-shell, such as certain diketopyrrolopyrrole derivatives and donor–acceptor conjugated polymers with quinoid repeat units, can exhibit intermediate diradical character.[23–28] We also demonstrated that croconaine dyes, typically classified as closed-shell species, actually exhibited intermediate diradical character.[29] These dyes consisting of chalcogenopyrylium and five-membered oxocarbons (see Fig. 2A), displayed notable temperature-dependent magnetic properties due to their thermally accessible triplet states.

In addition to the croconaine dyes, chalcogenopyrylium-based squaraine dyes, that were four-membered oxocarbon analogues for the variable applications,[30–33] also exhibited intermediate diradical character.[34] Although we previously confirmed that the chalcogenopyrylium moiety influences the contribution of the diradical structure, the impact of the central oxyallyl structure on the diradical character remains unclear. Thioxyallyl derivatives, where sulphur atom replaces the oxygen atom in the oxyallyl structure, are known to exhibit diradical character, unlike oxyallyl derivatives.[35] Therefore, investigating the effect of sulphur-substitutions in the central skeleton on diradical character of squaraine dyes is of particular interest.

In this study, we synthesized novel chalcogenopyrylium-based squaraine dyes featuring a cyclobutenedithione central skeleton (**SQ2a**: X = O, **SQ2b**: X = S) to evaluate their intermediate diradical character (Fig. 2B). These dyes exist as *cis–trans* isomers, where their intermediate diradical character is likely to influence the isomerization behavior. To investigate this further, we examined the *cis–trans* isomerization of the obtained dyes and compared their behaviour with existing squaraine dyes containing cyclobutenediones (**SQ1a–b**).

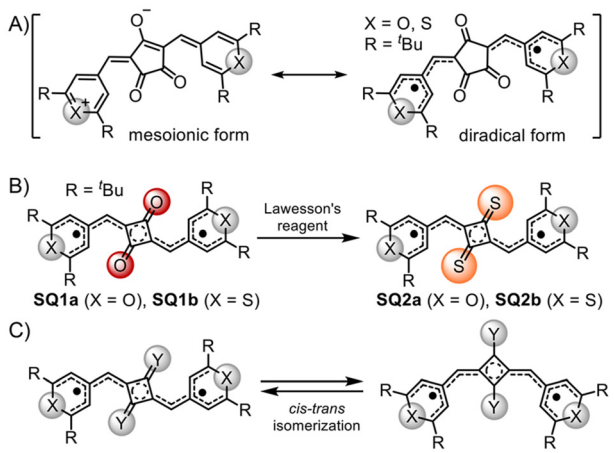

Fig. 2 (A) A resonance structure contributed by a diradical form of croconaine dyes consisting of a 5-membered oxocarbon moiety and chalcogenopyryliums. (B) Chalcogenopyrylium-based squaraine dyes with cyclobutenedithione moiety (**SQ2a–b**) synthesized from corresponding cyclobutenedione analouges (**SQ1a–b**). (C) Thermal *cis–trans* isomerization of the series of squaraine dyes.

Results and discussion

SQ2a and **SQ2b** were synthesized by thionation of precursor dye **SQ1a** and **SQ1b** with cyclobutenedione, respectively, using Lawesson's reagent in moderate yields (77% for **SQ2a** and 74% for **SQ2b**, see ESI‡).[36] They are stable in the solid state even at high temperature and in solution under dark conditions (Fig. S1‡), allowing for reliable measurements of ^{1}H NMR, ESR, and electronic absorption spectra.

Fig. 3 displays the X-ray structures of **SQ2a** and **SQ2b**, with detailed information available in the ESI.‡ Both dyes were analysed as planar *trans* isomers. In the crystal structure of **SQ2a**, two crystallographically independent molecules are present. We investigated the degree of diradical character by examining four major resonance forms (α to δ) chosen from 16 possible resonance forms (Fig. 3C, and Fig. S3‡). To evaluate their contribution, we analysed the difference in average bond lengths along the thio-oxyallyl part, denoted as ΔD = ave(g, p) − ave(h, q), where ave(a, b) represents the average of bond lengths a and b. For closed-shell mesoionic structures (α and β), ΔD = 0 due to identical bond lengths in the double and single bond pairs (g, p) and (h, q). In contrast, for the diradical δ form, ΔD > 0 because the outer parts (g and p) are single bonds while the inner parts (h and q) are double bonds. The γ form shows the reverse trend with ΔD < 0. Importantly, the ΔD values from the X-ray structures of **SQ2a** and **SQ2b** are positive (ΔD > 0), suggesting that the large contribution of diradical δ form, with unpaired electrons on the chalcogenopyrylium components (Table 1).

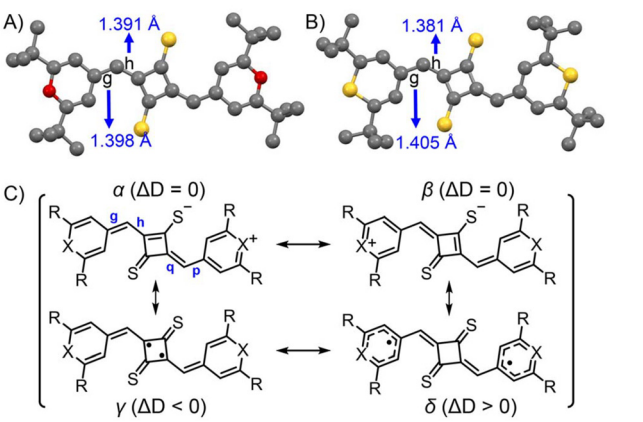

Fig. 3 Single crystal X-ray structures of **SQ2a** (A) and **SQ2b** (B) at 100 K. Bond lengths of the methine part (g and p) are shown in the Table 1. Resonance contributors of mesoionic structures (α and β), thio-oxyallyl diradical (γ), and chalcogenopyranyl radical (δ) (C). ΔD is defined as ΔD = ave(g, p) − ave(h, q).

Table 1 Bond length difference ΔD for singlet and triplet states of present squaraine dyes

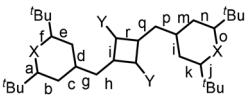

	ΔD = ave(g, p) − ave(h, q)		
Dye	Singlet[a]	XRD	Triplet[a]
SQ2a (X = O, Y = S)	0.004	0.002/0.007	0.030
SQ2b (X = Y = S)	0.011	0.024	0.039

[a] Obtained from optimized structures at the UB3PW91/cc-pVDZ level.

The singlet diradical nature of **SQ2a–b** was also confirmed by DFT calculations (see ESI, Table S3‡).[37–40] The ΔD value obtained from the crystal structure was intermediate between the values for the singlet and triplet states from DFT-optimized structures at the UB3PW91/cc-pVDZ level (Table 1). This suggests that **SQ2a–b** is in a state that lies between a pure singlet and triplet state.

The diradical index y_0, where $y_0 = 0$ and $y_0 = 1$ correspond to a perfect closed-shell and an open-shell electronic structure, respectively, is commonly used to express the degree of contribution of the diradical form in singlet diradicaloids (see ESI‡).[41] We estimated y_0 values for *trans* isomers of **SQ2a** and **SQ2b** using the spin-projected unrestricted Hartree–Fock (PUHF) theory using the 6-31G(d,p) basis set, obtaining values of 0.24 and 0.37, respectively (Table 2). These results suggest that the thiopyrylium skeleton enhances the contribution of the diradical form.

In addition to the bond length analyses, ESR spectra of these dyes displayed a signature of singlet diradicaloids. While the signal intensity of **SQ2a** was very low, both **SQ2a** and **SQ2b** exhibited signals with g values of 2.006, indicating the presence of carbon-centred radicals (Fig. 4). While **SQ2a** displayed negligible temperature-dependent behaviour, **SQ2b** showed increased signal intensity with rising temperature, indicating a thermal transition from singlet to triplet states that reflects its singlet diradical nature. This observation suggests that the thiopyrylium skeleton likely enhances the diradical contribution.

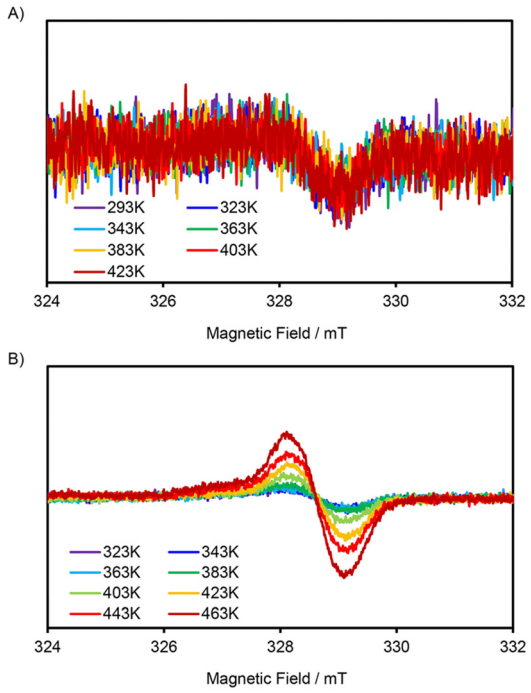

Fig. 4 ESR spectra of **SQ2a** (A) and **SQ2b** (B) in the solid state.

Unlike metal-free organic dyes with closed-shell structures, **SQ2a–b** exhibit characteristic temperature-dependent behavior in their ^{1}H NMR spectra in DMSO-d_6 due to their diradical character (Fig. 5A for **SQ2a**, Fig. 5B for **SQ2b**). At 303 K, **SQ2a** showed signals attributed to the proton on the pyrylium component. As the temperature increased, the signal broadened and completely disappeared at 333 K (Table 2). In **SQ2b**, no signal corresponding to the proton on the thiopyrylium components was observed, even at 303 K, where DMSO-d_6 barely freezes. These results indicate an increase in thermally excited triplet species with increasing temperature, confirming the intermediate diradical nature of **SQ2a–b**. Thus, ^{1}H NMR studies, along with ESR data, clearly show that the intermediate diradical character of **SQ2b** is higher than that of **SQ2a**.

We previously reported that **SQ1a–b**, with cyclobutenedione skeletons (precursors to **SQ2a–b**), also exhibits intermediate diradical character. For **SQ1a–b**, the proton signals disappear

Table 2 Indices associated with diradical character and *cis–trans* isomerization for **SQ2a**, **SQ2b**, **SQ1a**, and **SQ1b**

Dye	Signal-disappearance temperature in ^{1}H NMR [a]	Vibrational frequency (cm^{-1}) [b]	λ_{max} (nm) (log ε)[c]	$\Delta G^{\ddagger}$[d] (kcal mol^{-1})	y_0 [e]
SQ2a	333	1480	754 (5.22)	13.7	0.24
SQ2b	>303	1470	849 (5.28)	13.4	0.37
SQ1a	<423	1487	721 (5.37)	—	0.37
SQ1b	403	1478	822 (5.44)	14.5	0.47

[a] The temperatures at which the signals assigned to the protons of the chalcogenopyrylium skeleton disappear in DMSO-d_6. [b] Frequencies of the stretching bands around methine groups in $CHCl_3$. Details are shown in ESI.‡ [c] Electronic absorption maxima in DMSO. The values in parentheses indicate logarithm of molar absorptivity. [d] The Gibbs free energies of activation ($\Delta G^{\ddagger}$) for the *cis–trans* isomerization calculated by dynamic NMR method. Details are shown in ESI.‡ [e] The diradical index calculated by the spin-projected unrestricted Hartree–Fock (PUHF) theory using the 6-31G(d,p) basis set. Details are shown in ESI.‡

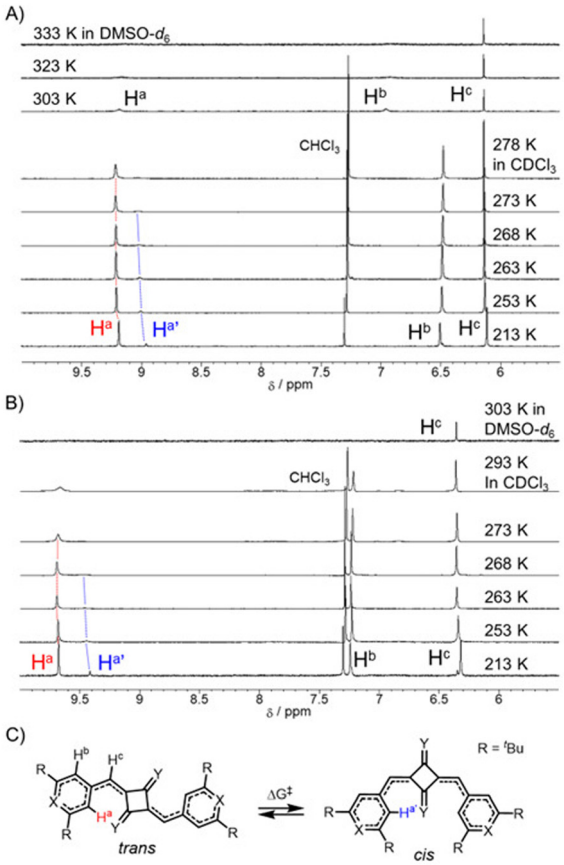

Fig. 5 (A) VT-^{1}H NMR spectra of **SQ2a** in DMSO-d_6 (333–303 K) and $CDCl_3$ (278–213 K). (B) VT-^{1}H NMR spectra of **SQ2b** in DMSO-d_6 (303 K) and $CDCl_3$ (293–213 K). (C) Schematic diagram of the thermal *cis–trans* isomerization and the Gibbs free energies of activation ($\Delta G^{\ddagger}$) for the isomerization.

above 400 K, whereas for **SQ2a–b**, the proton signals vanish at a lower temperature, around 300–330 K (Table 2). This is because **SQ2a–b** reach their thermally excited triplet state at a lower temperature, indicating a smaller energy gap between the singlet and triplet states and a significant contribution from the diradical forms. Thus, thionation of the central skeleton enhances the contribution of the diradical structure, even though the diradical index y_0 values for **SQ1a–b** are estimated to be larger than those for **SQ2a–b** due to limitations in computational accuracy.

The single crystal of **SQ1b** contains both *cis* and *trans* isomers, confirming that *cis–trans* isomerization occurs in solution.[42] Similar to **SQ1b**, **SQ2a–b** also exhibited *cis* and *trans* isomers at lower temperatures in $CDCl_3$ (Fig. 5A for **SQ2a**, Fig. 5B for **SQ2b** and Fig. S9–10‡ for **SQ1a–b**). Signals corresponding to the protons on the chalcogenopyrylium component coalesced at 278 K for **SQ2a** and at 273 K for **SQ2b**, suggesting that the isomerization is promoted at higher temperature condition and the signals for isomers is no longer observed in the NMR timescale. The Gibbs free energies of activation ($\Delta G^{\ddagger}$) for the *cis–trans* isomerization of **SQ2a** and **SQ2b** were estimated using the dynamic NMR method, resulting in values of 13.7 and 13.4 kcal mol^{-1}, respectively (Fig. 5C, and Table 2).[43] Although some error was introduced by the inability to observe peak shifts at temperatures below 213 K due to the freezing of $CDCl_3$ used in the measurements, **SQ2b**, with a cyclobutenedithione skeleton, exhibits a lower $\Delta G^{\ddagger}$ than **SQ1b**, which has a cyclobutenedione skeleton ($\Delta G^{\ddagger}$ = 14.5 kcal mol^{-1}).[44] The higher diradical contribution of **SQ2b** compared to **SQ1b** may lower the activation barrier and promote isomerization.

To measure the strength of the C–C double bond involved in isomerization, FT-IR spectra of these dyes in $CHCl_3$ were recorded. The IR absorption corresponding to the stretching vibration around the methine group in **SQ2b** was observed at a lower wavenumber compared to **SQ2a**, indicating that the bond in the methine group of **SQ2b** is relatively weaker (Table 2, Fig. S11 and 12‡). Thus, increased diradical character appears to diminish the double bond character of the methine group in the ground state, thereby promoting *cis–trans* isomerization.

The electronic absorption spectra for the dyes **SQ2a** and **SQ2b**, compared with those of **SQ1a** and **SQ1b**, are illustrated in Fig. 6 and summarized in Table 2. **SQ2a** and **SQ2b** each exhibit strong and sharp absorption peaks at 754 nm and 849 nm, respectively. The dyes with the cyclobutenedithione skeleton (**SQ2a**, **SQ2b**) exhibited absorption bands in a longer wavelength region compared to those with corresponding cyclobutenedione analogues (**SQ1a**, **SQ1b**). Notably, **SQ2b**, which has a high contribution from the diradical structure, demonstrated a lower transition energy. This is consistent with our previous results that a greater diradical character results in reduced transition energy according to the perturbation theory proposed by Fabian *et al.*[34,45] We also examined the temperature-dependence in absorption spectra of these dyes (Fig. 6B, and Fig. S15‡). With increasing temperature, the absorption bands of **SQ2a** and **SQ2b** were red-shifted by 2 nm and 5 nm, respectively. This change in absorption band with temperature might be attributed to *cis–trans* isomerization. DFT calculations estimate that the transition energy of the *cis* isomer is slightly lower than that of the *trans* isomer, suggesting that the equilibrium shifts towards the *trans* isomer at low temperatures due to *cis–trans* isomerization (Table S3 and S4‡).

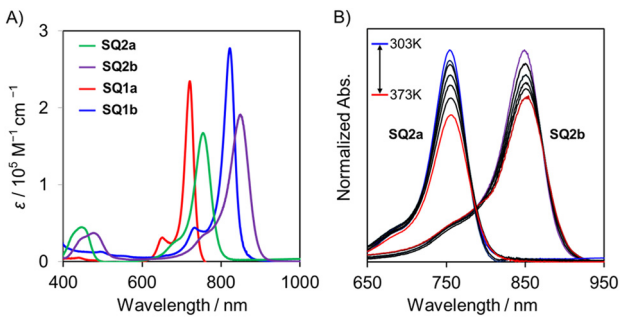

Fig. 6 (A) The electronic absorption spectra of **SQ2a** (green), **SQ2b** (purple), **SQ1a** (red) and **SQ1b** (blue) in DMSO (5 μM). (B) Normalized electronic absorption spectra of **SQ2a** and **SQ2b** in the temperature range from 373 to 303 K.

Conclusions

In summary, we synthesized cyclobutenedithione-based dyes **SQ2a–b** and analysed their intermediate diradical character using ^{1}H NMR, ESR, and theoretical calculations. Our results reveal that dyes incorporating a thiopyrylium component exhibit large degree of diradical character compared to those with a pyrylium component. Furthermore, **SQ2a–b** demonstrate a higher degree of diradical character than their cyclobutenedione counterparts (**SQ1a–b**). This enhanced diradical character promotes *cis–trans* isomerization, which is attributed to the weakening of the C–C double bonds involved. Additionally, **SQ2a–b** show subtle temperature-dependent changes in their electronic absorption spectra within the near-infrared region. Our study exemplifies the impact of diradical character on the physical and chemical properties of squaraine dyes, offering valuable insights for the design of advanced near-infrared absorbing dyes.

Data availability

The data supporting this article have been included as part of the ESI.‡ Crystallographic data for **SQ2a, SQ2b, SQ1a,** and **SQ1b** are available in the CCDC under deposit numbers 2382744, 2382745, 2194625 and 2194626,‡ respectively.

Conflicts of interest

There are no conflicts to declare.

Acknowledgements

This work was supported by JSPS KAKENHI Grant Numbers 24K01573, ENEOS Tonengeneral Research/Development Encouragement & Scholarship Foundation, Iketani Science and Technology Foundation, and JST, the Establishment of University Fellowships Towards the Creation of Science Technology Innovation, Grant Number JPMJFS2138.

References

1 M. Abe, Diradicals, *Chem. Rev.*, 2013, **113**, 7011–7088.
2 T. Kubo, Recent Progress in Quinoidal Singlet Biradical Molecules, *Chem. Lett.*, 2015, **44**, 111–122.
3 T. Y. Gopalakrishna, W. Zeng, X. Lu and J. Wu, From open-shell singlet diradicaloids to polyradicaloids, *Chem. Commun.*, 2018, **54**, 2186–2199.
4 H. Hayashi, J. E. Barker, A. Cárdenas Valdivia, R. Kishi, S. N. MacMillan, C. J. Gómez-García, H. Miyauchi, Y. Nakamura, M. Nakano, S. Kato, M. M. Haley and J. Casado, Monoradicals and Diradicals of Dibenzofluoreno [3,2-*b*]fluorene Isomers: Mechanisms of Electronic Delocalization, *J. Am. Chem. Soc.*, 2020, **142**, 20444–20455.
5 Q. Jing, T. Tao, H. Phan, Y. Han, T. Y. Gopalakrishna, T. S. Herng, G. Li, L. Yuan, J. Ding and C. Chi, Diazuleno-*s*-indacene Diradicaloids: Syntheses, Properties, and Local (anti)Aromaticity Shift from Neutral to Dicationic State, *Angew. Chem., Int. Ed.*, 2018, **57**, 16737–16741.
6 J. J. Dressler, M. Teraoka, G. L. Espejo, R. Kishi, S. Takamuku, C. J. Gomez-Garcia, L. N. Zakharov, M. Nakano, J. Casado and M. M. Haley, Thiophene and its sulfur inhibit indenoindeno-dibenzothiophene diradicals from low-energy lying thermal triplets, *Nat. Chem.*, 2018, **10**, 1134–1140.
7 W. Zeng, T. Y. Gopalakrishna, H. Phan, T. Tanaka, T. S. Herng, J. Ding, A. Osuka and J. Wu, Superoctazethrene: An Open-Shell Graphene-like Molecule Possessing Large Diradical Character but Still with Reasonable Stability, *J. Am. Chem. Soc.*, 2018, **140**, 14054–14058.
8 V. G. Jiménez, P. Mayorga-Burrezo, V. Blanco, V. Lloveras, C. J. Gómez-García, T. Šolomek, J. M. Cuerva, J. Veciana and A. G. Campaña, Dibenzocycloheptatriene as end-group of Thiele and tetrabenzo-Chichibabin hydrocarbons, *Chem. Commun.*, 2020, **56**, 12813–12816.
9 T. Nishiuchi, S. Aibara, H. Sato and T. Kubo, Synthesis of π-Extended Thiele's and Chichibabin's Hydrocarbons and Effect of the π-Congestion on Conformations and Electronic States, *J. Am. Chem. Soc.*, 2022, **144**, 7479–7488.
10 Y. Hayashi, S. Suzuki, T. Suzuki and Y. Ishigaki, Dibenzotropylium-Capped Orthogonal Geometry Enabling Isolation and Examination of a Series of Hydrocarbons with Multiple 14π-Aromatic Units, *J. Am. Chem. Soc.*, 2023, **145**, 2596–2608.
11 T. Takahashi, K. Matsuoka, K. Takimiya, T. Otsubo and Y. Aso, Extensive quinoidal oligothiophenes with dicyanomethylene groups at terminal positions as highly amphoteric redox molecules, *J. Am. Chem. Soc.*, 2005, **127**, 8928–8929.
12 R. P. Ortiz, J. Casado, V. Hernandez, J. T. López Navarrete, P. M. Viruela, E. Orti, K. Takimiya and T. Otsubo, On the Biradicaloid Nature of Long Quinoidal Oligothiophenes : New Experimental Evidences Guided by Theoretical Studies, *Angew. Chem., Int. Ed.*, 2007, **46**, 9057–9061.
13 J. Casado and J. T. López Navarrete, The longest quinoidal oligothiophene: a Raman story, *Chem. Rec.*, 2011, **11**, 45–53.
14 Q. Jiang, H. Wei, X. Hou and C. Chi, Circumpentacene with Open-Shell Singlet Diradical Character, *Angew. Chem., Int. Ed.*, 2023, **62**, e202306938.
15 Y. Yano, N. Mitoma, H. Ito and K. Itami, Correction to A Quest for Structurally Uniform Graphene Nanoribbons: Synthesis, Properties, and Applications, *J. Org. Chem.*, 2021, **86**(5), 4372–4373.
16 K. Kamada, K. Ohta, T. Kubo, A. Shimizu, Y. Morita, K. Nakasuji, R. Kishi, S. Ohta, S.-I. Furukawa, H. Takahashi and M. Nakano, Strong two-photon absorption of singlet diradical hydrocarbons, *Angew. Chem., Int. Ed.*, 2007, **46**, 3544–3546.
17 K. Kamada, S. Fuku-en, S. Minamide, K. Ohta, R. Kishi, M. Nakano, H. Matsuzaki, H. Okamoto, H. Higashikawa, K. Inoue, S. Kojima and Y. Yamamoto, Impact of Diradical Character on Two-Photon Absorption: Bis(acridine) Dimers

Synthesized from an Allenic Precursor, *J. Am. Chem. Soc.*, 2013, **135**, 232–241.
18 K. S. Mayer, D. J. Adams, N. Eedugurala, M. M. Lockart, P. Mahalingavelar, L. Huang, L. A. Galuska, E. R. King, X. Gu, M. K. Bowman and J. D. Azoulay, Topology and ground state control in openshell donor-acceptor conjugated polymers, *Cell Rep. Phys. Sci.*, 2021, **2**, 100467.
19 W. Chao, H. Hua and K. Tajima, Essential Role of Triplet Diradical Character for Large Magnetoresistance in Quinoidal Organic Semiconductor with High Electron Mobility, *Adv. Sci.*, 2022, **9**, 2201045.
20 H. Zhang, H. Phan, T. S. Herng, T. Y. Gopalakrishna, W. Zeng, J. Ding and J. Wu, Conformationally Flexible Bis (9-fluorenylidene)porphyrin Diradicaloids, *Angew. Chem., Int. Ed.*, 2017, **56**, 13484–13488.
21 M. Kozaki, A. Isoyama and K. Okada, Detection of a diradical intermediate in the cis–trans isomerization of 5,5′-bis (4,5-diphenyl-2*H*-imidazol-2-ylidene)-5,5′-dihydro-$\Delta^{2,2'}$-bithiophene, *Tetrahedron Lett.*, 2006, **47**, 5375–5378.
22 J. Wang, X. Xu, H. Phan, T. S. Herng, T. Y. Gopalakrishna, G. Li, J. Ding and J. Wu, Stable Oxindolyl-Based Analogues of Chichibabin's and Müller's Hydrocarbons, *Angew. Chem., Int. Ed.*, 2017, **56**, 14154–14158.
23 W. Wang, L. Ge, G. Xue, F. Miao, P. Chen, H. Chen, Y. Lin, Y. Ni, J. Xiong, Y. Hu, J. Wu and Y. Zheng, Fine-tuning the diradical character of molecular systems *via* the heteroatom effect, *Chem. Commun.*, 2020, **56**, 1405–1408.
24 Z. Chen, W. Li, M. A. Sabuj, Y. Li, W. Zhu, M. Zeng, C. S. Sarap, M. M. Huda, X. Qiao, X. Peng, D. Ma, Y. Ma, N. Rai and F. Huang, Evolution of the electronic structure in open-shell donor-acceptor organic semiconductors, *Nat. Commun.*, 2021, **12**, 5889.
25 Z. Chen, W. Li, Y. Zhang, Z. Wang, W. Zhu, M. Zeng and Y. Li, Aggregation-Induced Radical of Donor–Acceptor Organic Semiconductors, *J. Phys. Chem. Lett.*, 2021, **12**, 9783–9790.
26 T. L. D. Tam, G. Wu, S. W. Chien, S. F. V. Lim, S.-W. Yang and J. Xu, High Spin Pro-Quinoid Benzo[1,2-c;4,5-c′]bisthiadiazole Conjugated Polymers for High-Performance Solution-Processable Polymer Thermoelectrics, *ACS Mater. Lett.*, 2020, **2**, 147–152.
27 L. Huang, N. Eedugurala, A. Benasco, S. Zhang, K. S. Mayer, D. J. Adams, B. Fowler, M. M. Lockart, M. Saghayezhian, H. Tahir, E. R. King, S. Morgan, M. K. Bowman, X. Gu and J. D. Azoulay, Open-Shell Donor–Acceptor Conjugated Polymers with High Electrical Conductivity, *Adv. Funct. Mater.*, 2020, **30**, 1909805.
28 H. Cai, H. Tang, T. Wang, C. Xu, J. Xie, M. Fu, X. Luo, Z. Hu, Y. Zhang, Y. Deng, G. Li, C. Liu, F. Huang and Y. Cao, An n-Type Open-Shell Conjugated Polymer with High-Spin Ground-State and High Intrinsic Electrical Conductivity, *Angew. Chem., Int. Ed.*, 2024, **63**, e202402375.
29 A. Rajca, Organic Diradicals and Polyradicals: From Spin Coupling to Magnetism?, *Chem. Rev.*, 1994, **94**, 871–893.
30 P. Sun, Q. Wu, X. Sun, H. Miao, W. Deng, W. Zhang, Q. Fan and W. Huang, J-Aggregate squaraine nanoparticles with bright NIR-II fluorescence for imaging guided photothermal therapy, *Chem. Commun.*, 2018, **54**(95), 13395–13398.
31 S. Maryala, D. Sato, S. S. Pandey, S. Hayase and T. Kato, Efficient near infrared fluorescence detection of elastase enzyme using peptide-bound unsymmetrical squaraine dye, *Bioorg. Med. Chem. Lett.*, 2017, **27**(17), 4024–4029.
32 C.-A. Shen, D. Bialas, M. Hecht, V. Stepanenko, K. Sugiyasu and F. Würthner, Polymorphism in Squaraine Dye Aggregates by Self-Assembly Pathway Differentiation: Panchromatic Tubular Dye Nanorods versus J-Aggregate Nanosheets, *Angew. Chem., Int. Ed.*, 2021, **60**, 11949–11958.
33 C.-L. Sun, Q. Liao, T. Li, J. Li, J.-Q. Jiang, Z.-Z. Xu, X.-D. Wang, R. Shen, D.-C. Bai, Q. Wang, S.-X. Zhang, H.-B. Fu and H.-L. Zhang, Rational design of small indolic squaraine dyes with large two-photon absorption cross section, *Chem. Sci.*, 2015, **6**, 761–769.
34 T. Maeda, T. Oka, D. Sakamaki, H. Fujiwara, N. Suzuki, S. Yagi, T. Konishi and K. Kamada, Unveiling a new aspect of oxocarbons: open-shell character of 4- and 5-membered oxocarbon derivatives showing near-infrared absorption, *Chem. Sci.*, 2023, **14**, 1978.
35 W. Ando, Y. Hanyu, T. Furuhata and T. Takata, Thioxyallyl ion from allene episulfide with acid, *J. Am. Chem. Soc.*, 1983, **105**, 6151–6152.
36 T. Ozturk, E. Ertas and O. Mert, Use of Lawesson's Reagent in Organic Syntheses, *Chem. Rev.*, 2007, **107**, 5210–5278.
37 D. López-Carballeira, D. Casanova and F. Ruipérez, Potential Use of Squarates and Croconates as Singlet Fission Sensitizers, *ChemPhysChem*, 2018, **19**, 2224–2233.
38 S. Pradhan, Y. Kurokawa and S. S. Pandey, Design and Synthesis of Novel NIR-Sensitive Unsymmetrical Squaraine Dyes for Molecular Photovoltaics, *Phys. Status Solidi A*, 2023, **220**, 2300145.
39 V. V. Kurdyukov, A. I. Tolmachev, M. L. Dekhtyar, Y. G. Vlasenko and A. N. Chernega, A.N. Synthesis, spatial structure and spectral properties of pyrylo-4 (thio) squaraines variously substituted in cyclobutene moiety (2015) Journal of Physical Organic Chemistry, *J. Phys. Org. Chem.*, 2015, **28**, 452–459.
40 S. Ito, T. Nagami and M. Nakano, Diradical Character Based Design for Singlet Fission of Condensed-Ring Systems with 4nπ Electrons, *J. Phys. Chem. Lett.*, 2016, **7**, 3925–3930.
41 K. Yamaguchi, T. Fueno and H. Fukutome, A molecular-orbital theoretical classification of reactions of singlet ground-state molecule, *Chem. Phys. Lett.*, 1973, **22**(3), 461–465.
42 The crystal structures of **SQ1a** and **SQ1b** are available in the CCDC under deposit numbers 2194625 and 2194626,‡ respectively.
43 H. Friebolin, *Basic One- and Two-Dimensional NMR Spectroscopy*, Willey-VCH, 1991, p. 309.
44 Unfortunately, the activation free energy of **SQ1a** could not be calculated because the signal for H^a in *cis*-**SQ1a** could not be identified.
45 J. Fabian and R. Zahradník, The Search for Highly Colored Organic Compounds, *Angew. Chem., Int. Ed. Engl.*, 1989, **28**, 677–694.